2023 IEEE Nanotechnology Materials and Devices Conference (NMDC) | 979-8-3503-3546-0/23/$31.00 ©2023 IEEE | DOI: 10.1109/NMDC57951.2023.10343972

Sputter-deposited β-Ga_2O_3 films with Al top electrodes for resistive random access memory technology*

Aman Baunthiyal[1], Jon-Olaf Krisponeit[1,2], Alexander Karg[1], Seyed Majid Mahdian[1], Marco Schowalter[1,2], Thorsten Mehrtens[1,2], Martin Eickhoff[1,2], Andreas Rosenauer[1,2]and Jens Falta[1,2]

***Abstract*— Gallium oxide (β-Ga_2O_3) has been considered as a promising candidate for non-volatile resistive switching devices. However, it has been challenging for various deposition techniques to grow crystalline gallium oxide on metal substrates acting as bottom electrode in vertically stacked devices. We studied the synthesis of crystalline β-Ga_2O_3 on Ru/Al_2O_3 substrates using radio-frequency (RF) magnetron sputtering and characterized the electrical properties of Al/Ga_2O_3/Ru devices with respect to the effect of deposition time and temperature. The obtained devices showed more than 70 consistent IV cycles and ON-OFF ratios of up to 10^3. With increasing temperature and thickness, enhanced stability was observed in the endurance and retention cycles. The resistive switching (RS) behavior in these devices seems to be related to the formation and rupture of oxygen vacancy filaments.**

I. INTRODUCTION

To overcome conventional semiconductor scaling limitations, numerous technologies have been introduced for the advancement of non-volatile memories (NVM). Among these, resistive random access memories (ReRAMs) have emerged as one of the most promising switching device due to simple fabrication and structure, high integration density, long retention time, fast switching, low power consumption, excellent scalability and compatibility with standard complementary metal oxide semiconductor (CMOS) memory devices [1].

In recent years, gallium oxide (β-Ga_2O_3), a wide bandgap semiconductor (4.9 eV), has been intensely investigated for the use in UV devices [2] and low and high-power electronics [3] due to its very large breakdown voltage (8 MV/cm) as well as in sensor applications [4] owing to its conductivity being sensitive to oxygen. Previous studies on resistive switching in gallium oxide revealed unipolar [5] and bipolar [6] switching effects and explored the influence of various growth and fabrication parameters: Dramatic changes were observed by in dependence on the oxygen concentration of active layer [7] as well as achieved by changes in the carrier concentration using Cr doping by [8]. Furthermore, the effect of different work function electrodes has been explored in order to control the switching polarity and characteristics and the conductivity of the films [6].

In this work, we focus on structural characteristics and resistive switching properties of Ga_2O_3 grown by radio frequency (RF) magnetron sputtering on Ru/Al_2O_3 with respect to the influence of growth temperature and layer thickness. Furthermore, the switching mechanism is explained based on different transport mechanisms.

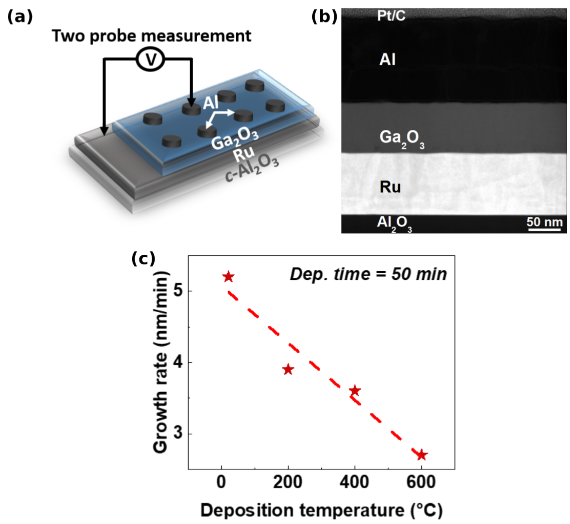

Fig. 1. (a) Schematic diagram of the Al/Ga_2O_3/Ru structure. (b) Cross-sectional TEM micrograph of the device. (c) Effect of deposition temperature on the growth rate of the gallium oxide films measured by XRR technique.

II. EXPERIMENTAL SECTION

Crystalline ruthenium films of approximately 100 nm thickness were prepared as a bottom electrode (BE) by radio frequency (RF) magnetron sputtering of a 3” ruthenium target at 450 °C with 30 W RF sputtering power onto (0001)-oriented Al_2O_3 substrates. Afterwards, the gallium oxide films were deposited on Ru/Al_2O_3 using the same technique at growth temperatures ranging from room temperature to 600 °C, with 40 W RF power. The deposition pressure was kept at 7×10^{-3} mbar. Finally, Al top electrodes (TE) of 500 µm diameter were deposited by e-beam deposition using a metal shadow mask to form the final Al/Ga_2O_3/Ru structure as shown in Fig. 1 (a) and (b).

The composition of gallium oxide films was analyzed using X-ray photoelectron spectroscopy (XPS) using an Omicron EA125 hemispherical analyzer. For each sample,

[1]Aman Baunthiyal, Jon-Olaf Krisponeit, Seyed Majid Mahdian, Alexander Karg, Marco Schowalter, Thorsten Mehrtens, Martin Eickhoff, Andreas Rosenauer and Jens Falta are with Institute of Solid State Physics, University of Bremen, Otto-Hahn-Allee 1, PO Box 330 440, 28359 Bremen, Germany (e-mail: baman@uni-bremen.de)

[2]Jon-Olaf Krisponeit, Marco Schowalter, Thorsten Mehrtens, Martin Eickhoff, Andreas Rosenauer and Jens Falta are with MAPEX Center for Materials and Processes, University of Bremen, PO Box 330 440, 28334 Bremen, Germany

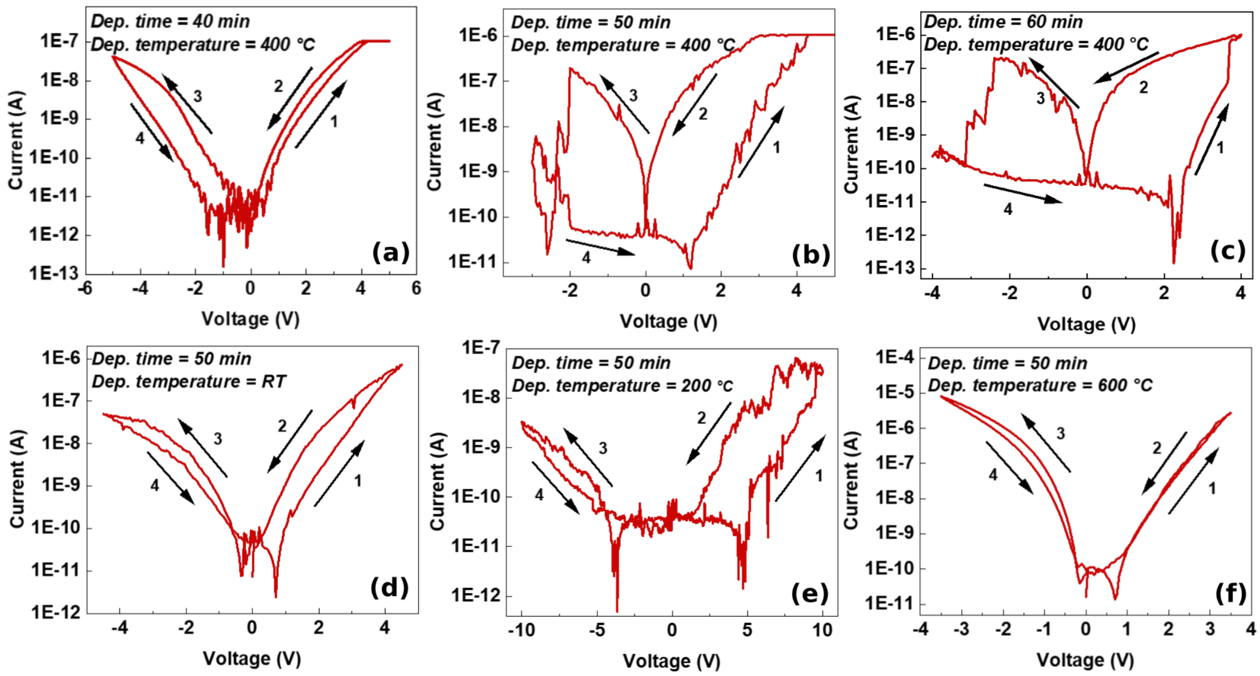

Fig. 2. IV characteristics of Al/Ga_2O_3/Ru devices in dependence on film thickness and deposition temperature. The upper row shows samples grown at 400 °C with different Ga_2O_3 deposition times and thicknesses: 40 min and (140 ± 10) nm (a), 50 min and (180 ± 10) nm (b), and 60 min and (220 ± 3) nm (c). At the bottom, the IV characteristics are shown for films grown at different temperatures for 50 min: RT (d), 200 °C (e), and 600 °C (f).

the film thickness was determined by X-ray reflectometry and the growth rates were calculated. Cross-sectional scanning transmission electron microscopy (STEM) was performed using a Thermo Fisher Spectra 30/300 (S)TEM. For electrical characterization, a Keithley 2450 source meter was employed at ambient conditions. During all electrical measurements, the Ru film was taken as a polarity reference.

III. RESULTS

In our previous research, we presented findings on the resistive switching behavior exhibited by (75 ± 3) nm Ga_2O_3 film grown using RF sputtering at 400 °C and 40 W sputtering power for 30 minutes [9]. This device type showed good ON/OFF ratio up to $> 10^3$ but poor endurance characteristics of < 40 AC voltage sweep cycles, reflecting a short device lifetime. Aiming for a better understanding and improved stability of the device grown at 400 °C, three devices with larger Ga_2O_3 thickness were prepared by varying the deposition time and investigated by the same technique. The film thicknesses of the new devices were (140 ± 10) nm, (180 ± 10) nm and (220 ± 3) nm as shown in Fig. 1 (c). The bipolar $I-V$ curves in Fig. 2 clearly demonstrate that the transition from the high resistive state (HRS) to the low resistive state (LRS) occurs at positive bias, while the transition from LRS to HRS found in negative bias. An increase in thickness to (140 ± 10) nm (Fig. 2 (a)) results in an overall increase in resistance for both HRS and LRS. However, the resistance increase in the HRS was not significant enough to clearly differentiate it from the LRS. In the device with a thickness of (180 ± 10) nm, a substantial increase in resistance for the HRS was observed, yielding a stable range of switching between the ON and OFF states with a ratio higher than 10^3 (see Fig. 2 (b)). However, when the thickness was further increased to (220 ± 3) nm, the ON/OFF ratio decreased by an order of magnitude accompanied by increased SET and RESET voltages. Both devices with thicknesses of (180 ± 10) nm and (220 ± 3) nm, showed more than 70 consistent IV cycles without any degradation of current in both states.

We also explored the effect of growth temperature on the growth rate and the RS stability. For this, three Ga_2O_3 films were deposited at room temperature, 200 °C, and 600 °C respectively, with a fixed deposition time of 50 minutes. It was observed that an increase in temperature leads to lower growth rate. The growth rates for these devices were $(5.2 \pm 0.2$ nm/min, (3.9 ± 0.2) nm/min and (2.7 ± 0.2) nm/min (see Fig. 1 (c)). Fig. 2 (d-f) illustrates the resulting current-voltage (IV) characteristics. The device grown at RT exhibited a higher thickness but lower resistance in both states compared to the 200 °C grown sample. We attribute this to a decrease in the concentration of electrically active defects, such as oxygen vacancies, with increasing temperature. When the thickness was decreased further at 400 °C growth temperature, the resistance decreased again for both states. As previously discussed, the device realized for these growth conditions exhibited the most favorable switching cycles, exhibiting a high ON/OFF ratio of approximately 10^3. Finally, a further increase in growth temperature to 600 °C, resulted in a suppression of the

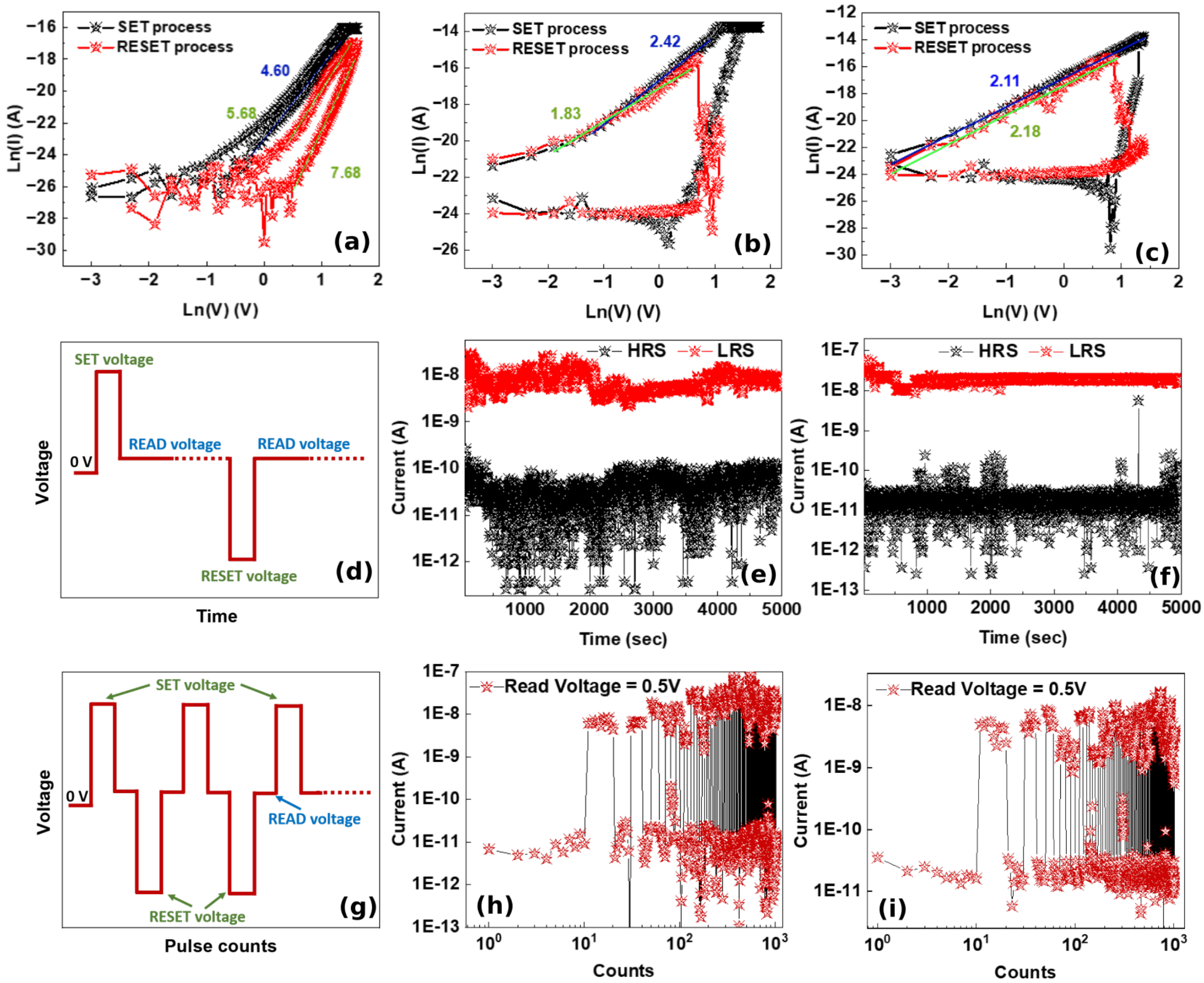

Fig. 3. Logarithmic IV characteristics of the Ga_2O_3 devices grown at 400 °C with different thicknesses: (140 ± 10) nm, (180 ± 10) nm, and (220 ± 3) nm (a–c, respectively). (d) Voltage pulse scheme for retention characteristics. (e) and (f) Retention characteristics of (180 ± 10) nm and (220 ± 3) nm Ga_2O_3 devices, respectively. (g) Voltage pulse scheme for endurance characteristics. (h) and (i) Endurance characteristics of (180 ± 10) nm and (220 ± 3) nm Ga_2O_3 devices measured at 0.5 V READ voltage.

switching effect. This may be attributed to a less defective growth of the Ga_2O_3 layer at higher temperature and, consequently, a lower concentration and mobility of the active defects.

In the logarithmic IV plots (Fig. 3 (a)-(d)), showing the characteristics of devices grown at 400°C, both HRS and LRS exhibit a non-linear voltage dependence on the current. As the resistance increases with thickness in both states, there is a corresponding change in slope, which also increases. To gain insights into the switching mechanism, several transport mechanism models such as Space Charge Limited Conduction (SCLC), Poole-Frenkel (PF) model, and Fowler-Nordheim tunneling were considered. Our previous research finding indicated that the (75 ± 3) nm thick device followed the Poole-Frenkel model in the HRS prior to transitioning to the LRS, where it displayed ohmic behavior [9].

Studying larger thicknesses, it became apparent that devices with (180 ± 10) nm and (220 ± 3) nm thicknesses exhibit a suppressed conduction at lower voltages. The slope for LRS for the thicker devices increased, demonstrating non-linear characteristics. The IV relationship can be divided into two regimes. In the lower voltage regime (<0.5V), the observed slope of $m = 1.82$ indicates that space charge limited conduction ($I \propto V^2$) governs the transport mechanism. In the higher voltage regime, the slope changes to $m = 2.42$, which can be associated with the equation $I \propto V^m$. The transport mechanism appears to involve trap-assisted hopping of charge carriers. The conduction path is contingent upon the presence of shallow traps/defects within the Ga_2O_3 film.

Retention and endurance refers to an examination of the stability of device with time. This assessment of resistance switching characteristics during electrical stress holds significant importance for the practical implementation of non-volatility in ReRAM devices. For retention characterization, both devices with thicknesses of (180 ± 10) nm and (220 ± 3) nm were effectively transformed from the HRS to the LRS, i.e. turned ON into the SET state. Subsequently, reading pulses of 0.5 V (on for 1 s, followed by off for 1 s) were consistently applied for 5000 s at room temperature. Following this, the device was reversed from LRS to HRS by applying negative voltage and the process was repeated in the HRS (device turned OFF) using the same read pulses scheme (see Fig. 3 (d)). For both devices, no current degradation was observed over time, resistances in both the HRS and the LRS remained stable throughout the 5000 s duration as shown in Fig. 3 (e) and (f). The relative noise amplitude of the current was higher in HRS due to the lower conductance.

To evaluate the cycle-to-cycle stability and reproducibility of both devices, electrical endurance tests were performed by applying AC square sweep pulses. The AC square voltage sweep consists of alternative SET and RESET potential, with a READ voltage measurement performed in between. Again, the read voltage for these measurements was set to 0.5 V at a pulse duration of 1s (see Fig. 3 (g)). Notably, both devices exhibit reliable endurance, maintaining the window of 10^3 for the (180 ± 10) nm device and 10^2 for the (220 ± 3) nm device (see Fig. 3 (h) and (i)). Throughout the measurement, no degradation of current was observed and and both states remained distinctly differentiable. Hence, the finding regarding the retention and endurance characteristics of both devices confirm the excellent and stable non-volatile properties, as well as clear differentiation between their HRS and LRS states.

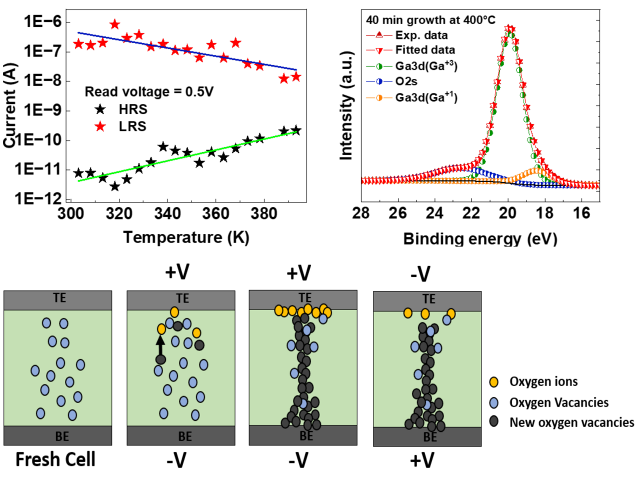

Fig. 4. (a) Temperature dependent variation of LRS and HRS current of the device. (b) XPS analysis of Ga3d peak of Ga_2O_3 at 400°C. (c) Schematic of the switching mechanism based on the formation of conductive filaments.

Furthermore, IV measurements were conducted at higher temperature. Fig. 4 (a) illustrates the resistances measured at a voltage of 0.5V. It is evident that the electrical transport properties of the device at LRS exhibit metallic behavior, i.e., the resistance increases with increasing temperature. Conversely, the device demonstrates semiconducting behavior in the HRS, with resistance decreasing as the temperature increases. Remarkably, there is no significant change in resistance over the measurement, indicating an exceptional stability of the device at elevated temperature.

The stoichiometry of the Ga_2O_3 films and concentration of oxygen vacancies were investigated using in-situ XPS. Fig. 4 (b) shows the Ga3d peak to comprise two subpeaks : (i) Ga^{+3} at 20 eV, associated to the Ga_2O_3 and (ii) Ga^{+1} at 18.4 eV, associated with suboxides. Therefore, the XPS analysis of the Ga3d peak reveals the presence of Ga-Ga metallic bonding and according oxygen vacancies. In our previous work, we discussed the interface between Al and Ga_2O_3, revealing the presence of an intermediate oxidic layer measuring approximately 5 nm [9]. We attributed the formation of the intermediate layer to the higher affinity of Al for oxygen. In a fresh cell, Al can attract oxygen ions, likely leading to the generation of additional defects in the GaO_x film near the interface. As the potential across the Ga_2O_3 film increases, the oxygen ions from the lattice sites can migrate towards the anode, resulting in the formation of more oxygen vacancies. These vacancies may arrange and create single or multiple small filaments within the device, which ultimately join together and transform the device from the HRS to the LRS. Applying a negative potential on Al is assumed to break the filament, as oxygen ions near to the interface between the TE (Al) and the Ga_2O_3 move towards the anode (i.e. Ru) and occupy the vacant sites near to the interface, effectively making the device open circuit and closing the switching cycle. A schematic of the proposed mechanism is shown in Fig. 4 (c).

IV. Conclusions

Ga_2O_3 based resistive-switching devices were fabricated on crystalline ultra-thin Ru films grown on sapphire with Alumunium top electrodes and examined by $I-V$ sweeps. The devices exhibit bipolar non-volatile switching characteristics. We explored the switching properties like resistance, ON/OFF ratio, and device stability with respect to the variation of the Ga_2O_3 thickness and growth temperature.

Devices grown at 400 °C featured the most stable switching behaviour, while other devices showed lower ON/OFF ratios ($< 10^1$ order). For higher Ga_2O_3 film thicknesses (180 nm and 220 nm) more stable switching behaviour was found in both retention and endurance cycles and ON/OFF ratios up to 10^3 and 10^2, respectively, were obtained. The presented sputter-deposited Ga_2O_3 based devices can hence be considered a promising candidate for future non-volatile memory technology.

Finally, a model for the underlying switching process was proposed in terms of a formation and rupture of conductive filaments. The differences in these devices may be attributed to an increase in the stability of the conductive filaments with increasing thickness.

References

[1] D. Kumar, R. Aluguri, U. Chand, T.Y. Tseng, "Metal oxide resistive switching memory: materials, properties and switching mechanisms," in *Ceramics International*, vol. 43, pp. S547-S556, Aug. 2017.

[2] X. Chen, F. Ren, S. Gu, and J. Ye, "Review of gallium-oxide-based solar-blind ultraviolet photodetectors," in *Photonics Research*, vol. 7, no. 4, pp. 381-415, Apr. 2019.

[3] M.J. Tadjer, ”Toward gallium oxide power electronics,” in *Science*, vol. 378, pp. 724-725, Nov. 2022.
[4] M. Fleischer, and H. Meixner, ”Gallium oxide thin films: a new material for high-temperature oxygen sensors,” in *Sensors and Actuators B*, vol. 4, no. 3-4, pp. 437-441, Jun. 1991.
[5] D.Y. Guo, Z.P. Wu, Y.H. An, P.G. Li, P.C. Wang, X.L. Chu, X.C. Guo, Y.S. Zhi, M. Lei, L.H. Li, and W.H. Tang, ”Unipolar resistive switching behavior of amorphous gallium oxide thin films for nonvolatile memory applications,” in *Applied Physics Letters*, vol. 106, no. 4, p. 042105, Jan. 2015.
[6] X. Gao, Y. Xia, J. Ji, H. Xu, Y. Su, H. Li, C. Yang, H. Guo, J. Yin, and Z. Liu, ”Effect of top electrode materials on bipolar resistive switching behavior of gallium oxide films,” in *Applied Physics Letters*, vol. 97, no. 19, p. 193501, Nov. 2010.
[7] J.J. Huang, T.C. Chang, J.B. Yang, S.C. Chen, P.C. Yang, Y.T. Chen, H.C. Tseng, S.M. Sze, A.K. Chu, and M.J. Tsai, ”Influence of oxygen concentration on resistance switching characteristics of gallium oxide,” in *IEEE electron device letters*, vol. 33, no. 10, pp. 1387-1389, Aug. 2012.
[8] D.Y. Lee, and T.Y. Tseng, ”Forming-free resistive switching behaviors in Cr-embedded Ga2O3 thin film memories,” in *Journal of Applied Physics*, vol. 110, no. 11, p. 114117, Dec. 2011.
[9] A. Baunthiyal, J.-O. Krisponeit, M. Schowalter, T. Mehrtens, A. Karg, A. Rosenauer, M. Eickhoff, and J. Falta, ”Growth and characterization of sputter-deposited Ga_2O_3-based memristive devices” *Applied Physics Letters*, under review.